ACS OMEGA

http://pubs.acs.org/journal/acsodf

Article

Fabrication of Biobased Hydrophobic Hybrid Cotton Fabrics Using Molecular Self-Assembly: Applications in the Development of Gas Sensor Fabrics

Ayyapillai Thamizhanban, Guru Prasanth Sarvepalli, Krishnamoorthy Lalitha, Yadavali Siva Prasad, Dinesh Kumar Subbiah, Apurba Das, John Bosco Balaguru Rayappan,* and Subbiah Nagarajan*

Cite This: *ACS Omega* 2020, 5, 3839−3848

Read Online

ACCESS | Metrics & More | Article Recommendations

ABSTRACT: Inadvertent inhalation of various volatile organic compounds during industrial processes, such as coal and metal mining, metal manufacturing, paper and pulp industry, food processing, petroleum refining, and concrete and chemical industries, has caused an adverse effect on human health. In particular, exposure to trimethylamine (TMA), a fishy odor poisonous gas, resulted in numerous health hazards such as neurotoxicity, irritation in eyes, nose, skin, and throat, blurred vision, and many more. According to the environmental protection agency, TMA in the level of 0.10 ppm is generally considered as safe, and excess dose results in "trimethylaminuria" or "fish odor syndrome." In order to avoid the health hazards associated with the inhalation of TMA, there is an urge to design a sensor for TMA detection even at low levels for use in food-processing industries, medical diagnosis, and environment. In this report, for the first time, we have developed a TMA sensor fabric using a sequential self-assembly process from silver-incorporated glycolipids. Formation of self-assembled supramolecular architecture, interaction of the assembled structure with the cotton fabric, and sensing mechanism were completely investigated with the help of various instrumental methods. To our surprise, the developed fabric displayed a transient response for 1−500 ppm of TMA and a stable response toward 100 ppm of TMA for 15 days. We believe that the reported flexible TMA sensor fabrics developed via the sequential self-assembly process hold great promise for various innovative applications in environment, healthcare, medicine, and biology.

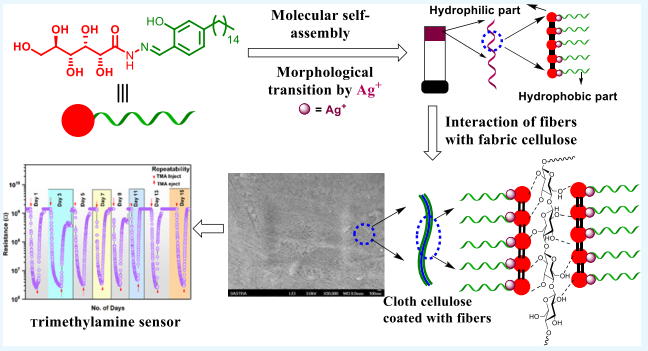

1. INTRODUCTION

Emission of toxic gases and volatile organic compounds (VOCs) into the atmosphere from industries, evaporation of organic solvents, petroleum products, and other human activities are a grave threat to living organisms. Emission of VOCs causes many health hazards owing to their vital role in many photochemical reactions, forming harmful products with toxic, carcinogenic, and mutagenic properties.[1]ence, detection of VOCs has become a frontline research in recent years, and there is a huge demand for the development of sensors for VOCs. Among the various VOCs, trimethylamine (TMA, C_3H_9N) is a type of colorless, flammable, fishy odor, and poisonous gas, which is generated naturally during the intestinal biodegradation of choline and carnitine rich foods such as fish, egg yolk, soybeans, peas, and so forth and during the biodegradation of damp building material, plants, fish, and other sea food and animal products.[2−5] Exposure to even a trace amount of TMA vapor can cause irritation of the eyes, nose, skin, throat, and respiratory system as well as vomiting, cough, dyspnea, blurred vision, difficulty in swallowing, head ache, abdominal pain, and neurotoxicity.[6] Excessive accumulation of TMA in the body fluids leads to "trimethylaminuria" or "fish odor syndrome." Nevertheless, there is an urge to develop a facile sensor to detect TMA for use in food-processing industries, medical diagnosis, and environment.

Traditionally, various analytical methods such as gas chromatography, liquid chromatography, and ion mobility spectrometry were employed to detect TMA vapors. Recently, chemical gas sensors based on semiconducting metal oxides were used because of its rapid, high response, and cost-effective sensing. However, device fabrication, sensitivity, and selectivity are the foremost problems associated with the semiconducting metal oxide-based gas sensors. In order to overcome the existing limitation and to amplify the selectivity and sensitivity,

Received: August 24, 2019
Accepted: January 28, 2020
Published: February 12, 2020

https://dx.doi.org/10.1021/acsomega.9b02733
ACS Omega 2020, 5, 3839−3848

Scheme 1. One Pot Synthesis of Glycolipid 3

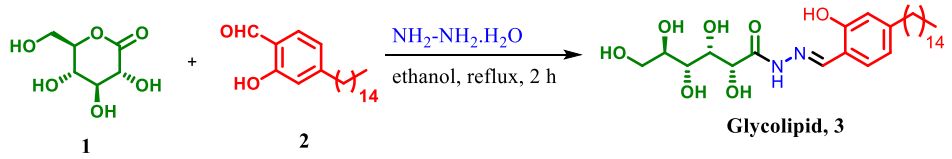

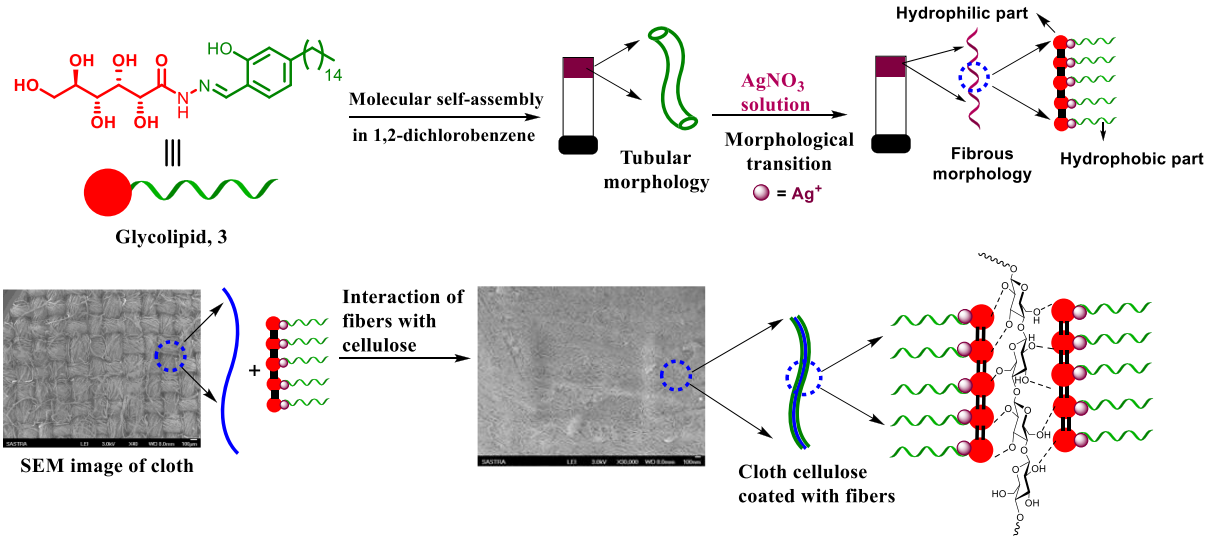

Figure 1. Pictorial representation of the formation of cotton fabric decorated with GL-AgNPs.

various efforts such as modulation of sensor temperature, doping with catalytic oxides, loading of noble-metal catalysts, and so forth were made.[2,7−13] Recent studies revealed that several metal-oxide sensors such as TiO_2,[12,14−16] ZnO,[17−19] MoO_3,[2,20−23] SnO_2,[24] and Fe_2O_3[25,26] and composites such as $ZnO−Al_2O_3/TiO_2/V_2O_5$,[27−29] $SnO_2−ZnO$,[30] $ZnO−Cr_2O_3$,[31] $ZnO−In_2O_3$,[32] and so forth have been used for TMA detection. However, the usage of gas sensors based on inorganic semiconductors results in the accumulation of metals in the environment and pose severe pollution at various levels. Recently, metal−organic frameworks (MOFs), the porous materials obtained via the self-assembly of organic ligands and inorganic metal ions or clusters, were used in various applications such as catalysis, gas storage and separation, drug delivery, sensing, and so forth owing to their structural flexibility and tunable porosity.[33−42] Chidambaram and Stylianou have highlighted the importance of MOFs and their potential to sense various gases and vapors such as alkanes, aldehydes, TMA, ammonia, hydrogen sulfide, and nitric oxide.[42] Interest toward the design and synthesis of functional molecules for the construction of molecular devices suitable for applications like drug delivery, catalysis, sensing, and forth has increased substantially. In this regard, for the first time, we report the formation of self-assembled silver-incorporated glycolipids, GL-AgNPs, using the sequential self-assembly process and explore the possibility of using them in constructing a conductive fabric for sensing TMA vapors.

2. RESULTS AND DISCUSSION

2.1. Synthesis. Interest toward the design, synthesis, and construction of functional molecules from renewable resources has augmented a lot as they could serve as molecular devices for sensing, switching, and signal selectivity. In this regard, we constructed a functional molecule for sensor application by synthesizing glycolipid **3** in good yield using a simple procedure involving the reaction of gluconolactone **1** (1.0 mmol) with hydrazine hydrate (1.5 mmol), followed by the addition of 2-hydroxy-4-pentadecylbenzaldehyde **2** (1.0 mmol) under reflux condition as reported in our previous work (Scheme 1).[43]

After the synthesis and complete characterization using nuclear magnetic resonance (NMR) spectrometry and mass spectral studies, the gelation ability of glycolipid **3** was examined in a wide range of solvents and oils using the "stable to inversion of a test tube" method. Interestingly, glycolipid **3** displayed gelation in a wide range of solvents with the minimum critical gelation concentration (CGC).[43] To our surprise, morphological analysis of the gel formed by glycolipid **3** in 1,2-dichlorobenzene (CGC = 0.5% w/v) displayed a helical tubular architecture, and the detailed investigation is reported elsewhere.[43] However, by getting clue from our recent results on the morphological transition from the helical tubules of the gel to the fibrous network architecture without even a change in the phase driven by metal ions, we have prepared assembled GL-NPs **4a−c**. A simple strategy for the synthesis of assembled nanomaterials has created great interest among the researchers. In particular, access to the finite nanoarchitecture via the coordination of metal to the self-assembled supramolecular system is rather limited.[45] On the most basic level, complementary small molecules assembled via intermolecular interactions, such as H-bonding, $\pi-\pi$ interactions, van der Waals forces, anion and cation−π interactions, and other weak interactions, having metal recognition sites share the concept of most emerging MOFs and supramolecular coordination complexes (SCCs). In this report, we present a metal-driven morphological transition in the supramolecular assembly of small molecules via the coordination to generate a

https://dx.doi.org/10.1021/acsomega.9b02733
ACS Omega 2020, 5, 3839−3848

hybrid system of MOF and SCC. In order to achieve the hybrid nanoarchitecture, a solution of silver nitrate, copper acetate, and zinc acetate solutions was added to the gel separately, displaying chiral helical tubules architecture formed by supramolecular assembly (Figure 1). The added metal ions interacted with the coordination site in the chiral helical tubules formed by compound **3** and further induced the morphological transition in the gel without any phase change and generated a MOF−SCC hybrid system (GL-NPs) displaying a fibrous structure. The supernatant solution on the MOF−SCC hybrid gel was decanted and completely air dried. The excess metal ions percolated in the fibrous structure of the gel was removed by washing it very well with cold ethanol and then dried. The dried GL-NPs were stored under desiccation and used for sensor studies. Among the various GL-NPs, such as GL-CuNPs, GL-ZnNPs, and GL-AgNPs, synthesized involving the concept of supramolecular assembly, GL-AgNPs displayed better sensitivity toward TMA vapors in the preliminary investigation. Based on the preliminary results, we have selected GL-AgNPs for the fabrication of a conductive fabric using the concept of intermolecular interactions. The dried self-assembled GL-AgNPs were dispersed uniformly into 1,2-dichlorobenzene by sonication, and a cotton fabric of 5 × 5 cm^2 was kept immersed in the dispersed solution of GL-AgNPs for about 24 h. The hydrophilic part of GL-AgNPs interacted with the cellulose in the cotton fabric and generated GL-AgNP-decorated cellulose (Figure 1). Self-assembly of GL-AgNPs on other fabrics, such as silk, wool, and polyester, were not successful because of the absence of free hydroxyl groups. Morphological transitions in self-assembled glycolipid **3** from tubular to fibrillar structure induced by Cu^{2+} and Zn^{2+} were reported elsewhere.[43] However, GL-AgNPs displayed better sensitivity and selectivity toward various gases when compared to GL-CuNPs and GL-ZnNPs. In the present study, we focus on the characterization and explore the possible potential applications of self-assembled GL-AgNPs and cotton fabric decorated with GL and GL-AgNPs.

Morphology of GL-AgNPs, pristine fabric, GL-coated fabric, and GL-AgNP-coated fabric were identified by the field emission scanning electron microscopy (FESEM) analysis (Figure 2). It can be seen from Figure 2a,b that the xerogel of GL-AgNPs displayed a three-dimensional (3D) fibrous network structure displaying width ranging from 200 to 400 nm.

Energy-dispersive X-ray elemental mapping of C, N, O, and Ag in GL-AgNPs is shown in Figure 2c, which reveals the uniform distribution of AgNPs in the fibrous architecture. Figure 2d,e reveals the existence of longitudinal smooth fibrils in the pristine fabric. FESEM images of fabric coated with xerogel of **3** is shown in Figure 2f,g, which clearly revealed the presence of helical tubes formed by the self-assembly of compound **3** in 1,2-dichlorobenzene on to the fabric surface. However, a uniform coating of GL-AgNPs on the cotton fabric was observed because of the H-bonding interaction between the hydrophilic part of fibrils and cellulose (Figure 2h−n). EDX elemental mapping of fabric coated with GL-AgNPs clearly indicated the uniform interaction of AgNPs with the cellulose of cotton fabric via H-bonding (Figure 2).

X-ray diffraction analysis was carried out to provide further justification for the formation of GL-AgNPs. The diffraction pattern of the xerogel of glycolipid **3** displayed periodic peaks at 2θ = 2.48, 4.96, 10.15, 15.24, and 20.43°,[43] whereas GL-AgNPs showed peaks at 3.19, 4.89, 6.15, 10.06, 15.19, 20.30, 21.66, 32.24, and 38.04° (Figure 3a). Morphological

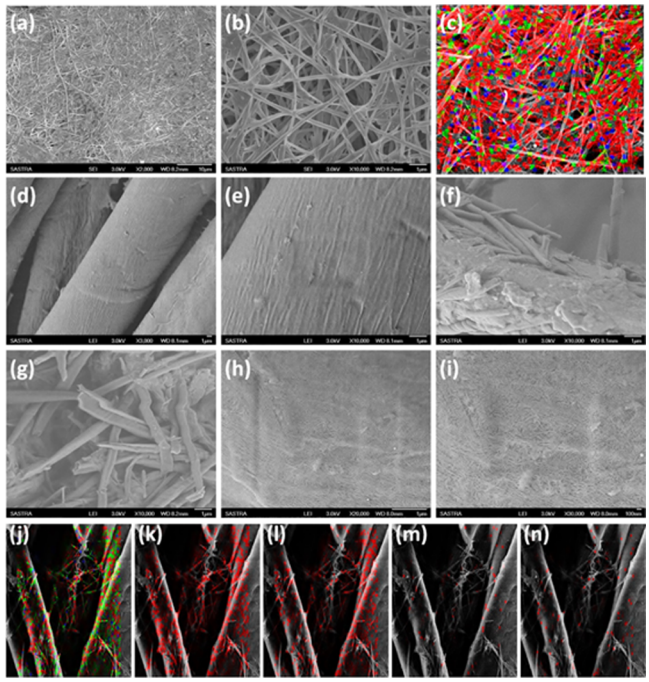

Figure 2. Morphological analysis of GL-AgNPs, pristine fabric, GL-coated fabric, and GL-AgNP-coated fabric using FESEM. (a,b) Xerogel of GL-AgNPs; (c) mapping of elements present in the GL-AgNPs xerogel using the energy-dispersive X-ray elemental mapping method; (d,e) micrographs of pristine cotton fabric; (f,g) fabric coated with well dispersed xerogel of **3** in 1,2-dichlorobenzene; (h−n) fabric coated with well dispersed GL-AgNPs in 1,2-dichlorobenzene; (j−n) elemental mapping of fabric coated with GL-AgNPs: (j) complete mapping of elements, (k) carbon, (l) oxygen, (m) nitrogen, and (n) silver.

transition-driven Ag^+ can be identified from the appearance of the peak at 2θ = 38.04° corresponding to the (111) plane of silver.[46] XRD diffraction analysis of the fabric and GL-AgNP-coated fabric also supports the existence of molecular self-assembly and the incorporation of AgNPs in the coated cloth surface (Figure 3b).[47]

X-ray photoelectron spectroscopy (XPS) is a surface-sensitive quantitative method which helps in establishing the elemental composition, the elements in the chemical and electronic states, and the nature of interaction existing in the system. In order to investigate the nature of interaction between AgNPs and fibrils of self-assembled glycolipid **3**, XPS spectral analysis of helical tubules of glycolipid **3** was performed, which displayed signals corresponding to C 1s, N 1s, and O 1s that on deconvolution revealed the existence of −C═C−/−C−C−/(285.2 eV), −C−O−/−C−N− (285.5 eV), and C═N (286.5 eV).[43] Figure 4 shows the XPS spectrum of xerogel of GL-AgNPs and their deconvolution. The deconvolution of C 1s of GL-AgNPs displayed peaks with binding energies (BEs) of 284.5 and 285.1 eV, which revealed the presence of −C═C−/−C−C−/−C−H and −C−O−/−C−N− (Figure 4b). The spectrum of N 1s showed peaks at 399.31 and 400.14, and O 1s displayed peaks at 532.2 and 532.8 eV (Figure 4c,d). The XPS spectra of Ag 3d showed two XPS signals at BEs of 368.3 and 374.1 eV with the separation of 6.0 eV corresponding to Ag $3d_{5/2}$ and Ag $3d_{3/2}$ BE of Ag^0, respectively (Figure 4e).[46,47]

The viscoelastic behavior and flow characteristics of the self-assembled material can be examined by performing rheological

https://dx.doi.org/10.1021/acsomega.9b02733
ACS Omega 2020, 5, 3839−3848

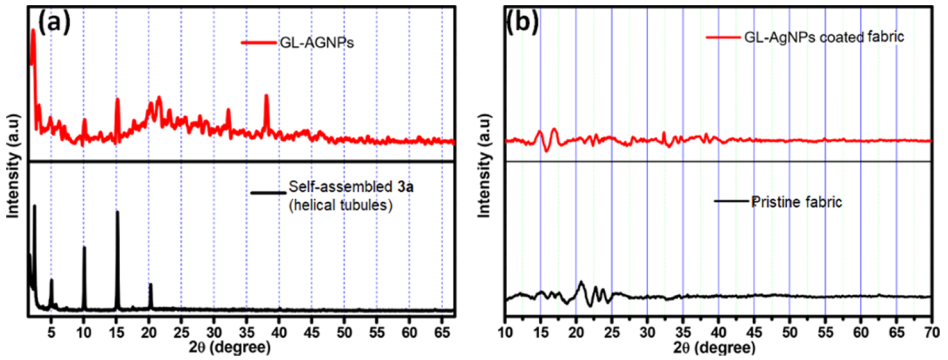

Figure 3. (a) XRD spectra of xerogel of self-assembled glycolipid **3a** and GL-AgNPs; (b) XRD spectra of pristine fabric and GL-AgNP-coated fabric surface. Reproduced from ref 43 with permission from The Royal Society of Chemistry.

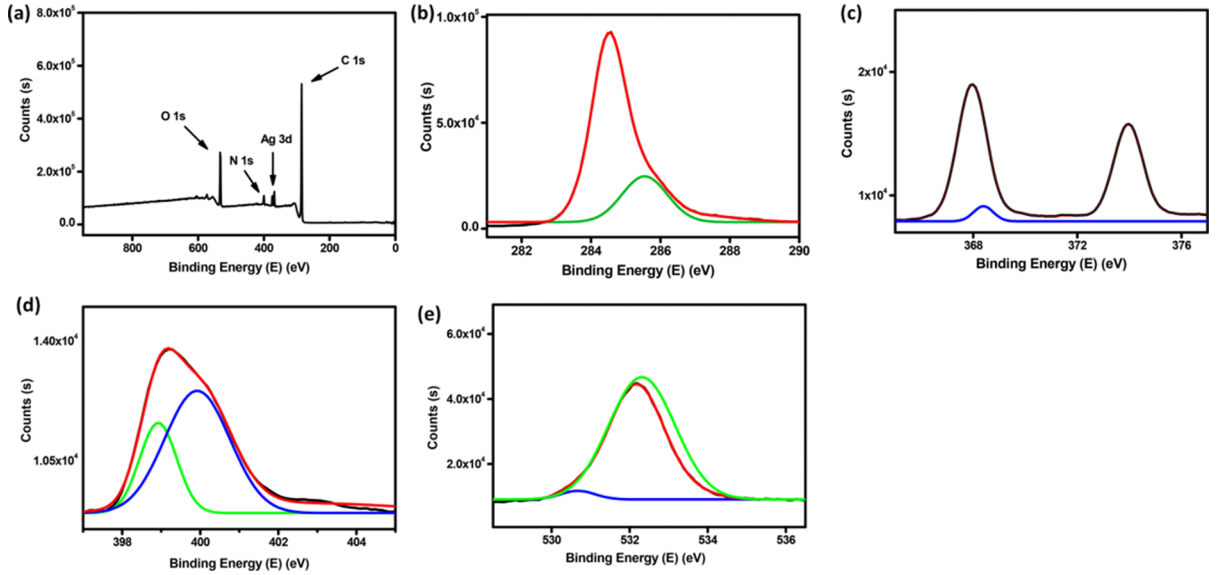

Figure 4. XPS spectra of (a−e) self-assembled GL-AgNPs fitted using Gaussian−Lorentzian peak: (a) self-assembled GL-AgNPs; (b) C 1s; (c) Ag 3d; (d) N 1s; and (e) O 1s spectra.

studies. In order to examine the mechanical strength of the GL-AgNP gel, a frequency sweep experiment was carried out by applying a constant strain of 1% at room temperature with respect to the storage modulus (G') and loss modulus (G''). During the entire range of frequency sweep, G' value was observed to be greater than G'', which clearly revealed the mechanical strength of the gel that is strong enough to tolerate the external forces (Figure 5a). The amplitude sweep experiment was performed to identify the critical strain (γ_c), the point up to which the self-assembled material tends to retain its structural integrity by exhibiting solid-like behavior and displays liquid-like behavior thereafter. The value of γ_c at which G' equals G'' was found to be 11.86% ($G' = G'' = 514.03$ Pa) (Figure 5b).

A gel is said to exhibit thixotropic behavior when it is capable of regenerating its gel network structure in the step strain experiment. During this experiment, the value of G' and G'' was found to decrease on applying a high magnitude of strain (100%), indicating the breaking of the gel network structure, and when the strain was reduced to 0.1%, recovery of G' and G'' was observed signifying the regeneration of the gel (Figure 5c). Continuous temperature ramp-up and ramp-down experiments clearly show the thermal processability of the GL-AgNP gel (Figure 5d).

After establishing the mechanical stability and processability of the GL-AgNP gel, we were curious to probe the surface of GL-AgNP-coated fabric. As per the mechanism proposed, after interaction of GL-AgNPs with the cellulose of cotton fabric via H-bonding, the fabric surface should display hydrophobicity. The wettability of the coated cloth surface was probed by measuring the contact angle at an ambient temperature using a goniometer. When a double-distilled water droplet was placed on the pristine cotton fabric, immediate absorption of water was observed, whereas for the fabric coated with GL-AgNPs, GL-CuNPs, and GL-ZnNPs, the static contact angles of 114.1, 125.4, and 136.0°, respectively, were observed, which indicate the hydrophobic nature of the coated surface irrespective of the metal ions used (Figure 6).

2.2. Gas-Sensing Characteristics. *2.2.1. Selectivity.* A pure cotton cellulose with yarn warp and weft count of 20.3 × 15.3 picks per inch was procured from the Department of Textile and Fibre Engineering, Indian Institute of Technology Delhi, New Delhi. The cotton fabric was used as a sensing substrate for fabricating the flexible gas sensor toward the detection of TMA. Prior to the fabrication process, the cotton substrates were pretreated with sodium hydroxide solution in order to remove impurities such as wax, grease, and other noncellulosic compounds. Because sensitivity, selectivity, and

https://dx.doi.org/10.1021/acsomega.9b02733
ACS Omega 2020, 5, 3839−3848

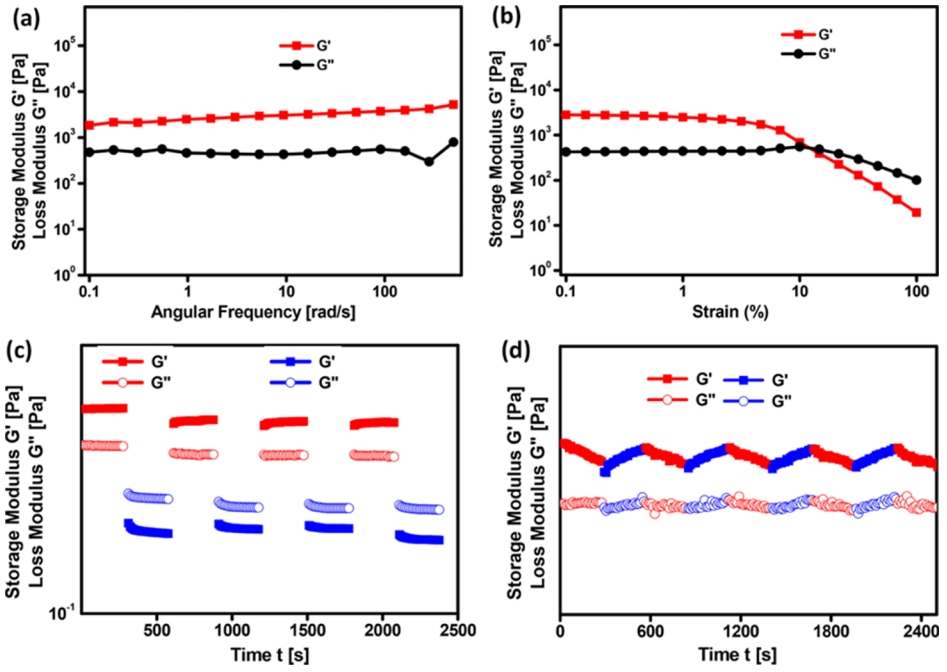

Figure 5. (a–d) Rheological behavior of GL-AgNPs gel formed in 1,2-dichlorobenzene. (a) Frequency sweep, (b) amplitude sweep, (c,d) step strain and continuous temperature ramp-up and ramp-down experiments, respectively. In the step strain experiment, a high strain of magnitude 100% (red line) and a low strain of magnitude 0.1% (blue line) were applied alternatively. Temperature ramp-up and ramp-down experiments for the gel is 25 to 45 °C (red line) and 45 to 25 °C (blue line).

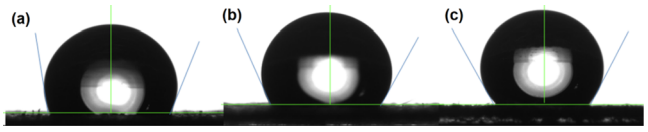

Figure 6. (a–c) Images displaying the contact angle of the fabric coated with (a) GL-AgNPs, (b) GL-CuNPs, and (c) GL-ZnNPs respectively.

stability are the key parameters to be considered while fabricating a sensor, the same parameters have been investigated and reported. Selectivities of GLNPs, GL-ZnNPs, GL-CuNPs, and GL-AgNPs surface-modified cotton fabrics were studied toward 100 ppm of ammonia (NH_3), formaldehyde (CH_2O), TMA, ethanol (C_2H_5OH), acetaldehyde (C_2H_4O), methanol (CH_3OH), and isopropanol (C_3H_8O) vapors at room temperature and are shown in Figure 7a. All GL-NP-modified cotton fabrics showed higher selectivity toward TMA with the incorporation of different metal ions on the GL-NP sensing element. The architecture of the sensing element is shown in Figure 7b. The response value of the sensing element is calculated using eq 1,

$$S = \frac{R_a}{R_g} \qquad (\text{if } R_a \gg R_g) \tag{1}$$

where R_a and R_g are the resistances of the surface-modified cotton fabric in an ambient air atmosphere and target gas atmosphere, respectively. Response/recovery time (τ_{res}/τ_{rec}) is defined as the time taken by the sensing element to attain 90% of change in the total surface resistance.

The selective response toward TMA might be due to the lower ionization energy and lower dipole moment than the other target analytes as given in the following order:[48] C_3H_9N

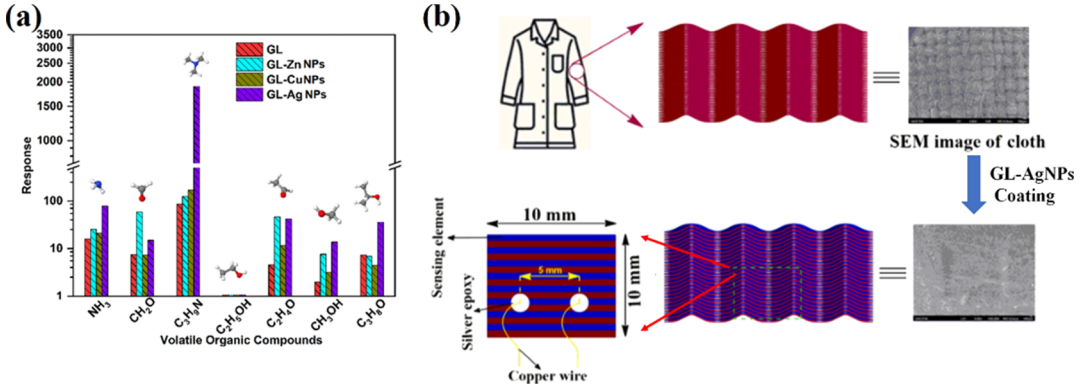

Figure 7. (a) Selectivity of surface-modified cotton fabrics with GLNPs, GL-ZnNPs, GL-CuNPs, and GL-AgNPs toward 100 ppm of ammonia, formaldehyde, TMA, ethanol, acetaldehyde, methanol, and isopropanol vapors; (b) gas sensor device architecture diagram with cross-section and dimensions.

https://dx.doi.org/10.1021/acsomega.9b02733
ACS Omega 2020, 5, 3839−3848

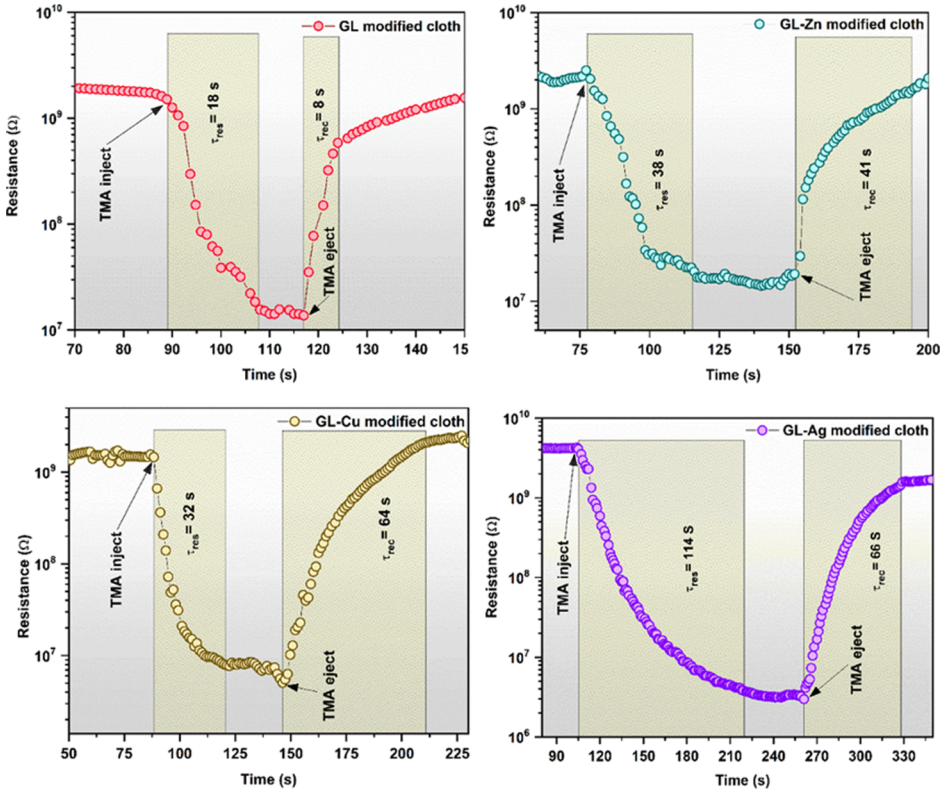

Figure 8. Transient responses of cotton fabrics modified with GLNPs, GL-ZnNPs, GL-CuNPs, and GL-AgNPs toward 100 ppm of TMA.

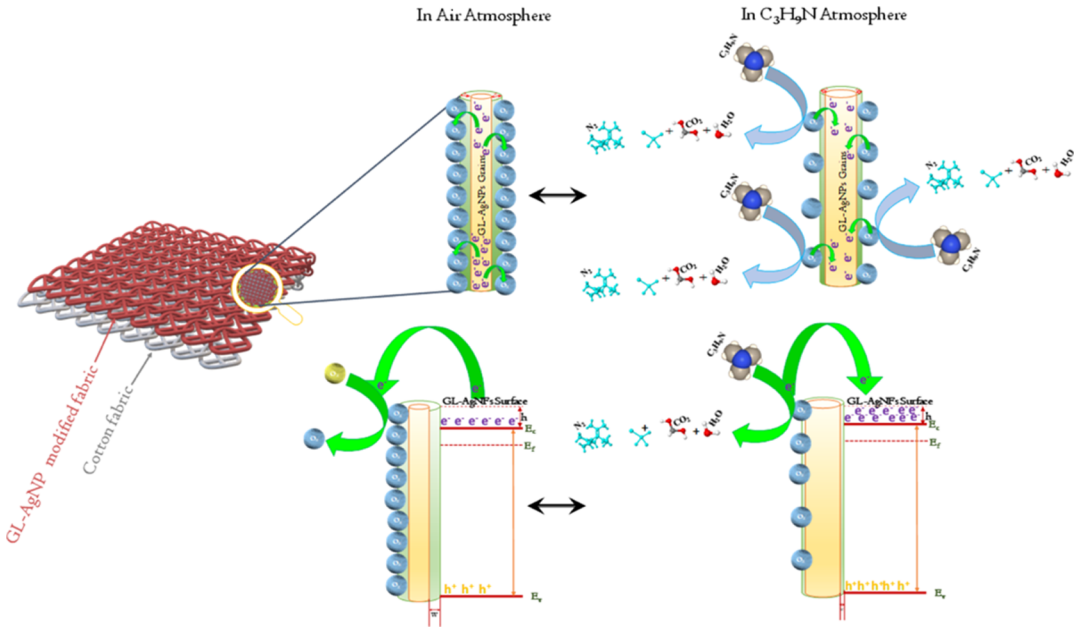

Figure 9. Schematic representation of the sensing mechanism of GL-AgNPs-modified cotton fabric in the presence of TMA vapor.

< C_3H_8O < NH_3 < C_2H_4O < C_2H_5OH < CH_3OH < CH_2O. Also, C_3H_9N (TMA) has stronger interaction with the sensing element than other targeted analytes because of its lower bond dissociation energy in comparison with other target analytes. In comparison, incorporation of the Ag metal complex with GLNPs showed a maximum sensing response of 1908 toward TMA. Because of the interaction of TMA with the GL-AgNPs-modified fabric through donation of 21 electrons by the amine groups to the chemisorbed oxygen species (eq 4), a greater change resulted in the surface resistance. Moreover, the sensing response of GLNPs (86), GL-ZnNPs (125), and GL-CuNPs (169) toward TMA was comparatively lower than that of GL-AgNPs-modified cotton fabric (1908). The incorporation of metal ions such as Ag, Cu, and Zn on GLNPs lead to the formation of covalent bonds with the amide group of glycolipids and resulted in the donation of electrons because of its hyperelectronic behavioral elements.[49] Also, the enhanced surface conductivity of GL-AgNPs surface-modified

https://dx.doi.org/10.1021/acsomega.9b02733
ACS Omega 2020, 5, 3839−3848

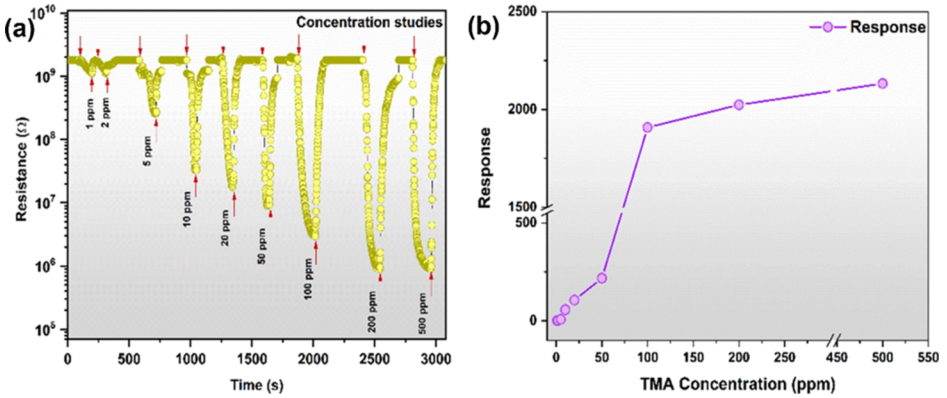

Figure 10. (a,b) Dynamic response and response trend of GL-AgNPs-modified cotton fabric toward 1−500 ppm of TMA.

cotton fabric compared to that of other metal compound-modified fabric might have resulted in increased sensing response toward TMA. In addition, incorporation of Ag metal on GLNPs provides a significant electron-transfer mechanism between the cations present in the glycolipid compound as Ag ↔ Ag^+. The transient responses of surface-modified cotton fabrics with GLNPs, GL-ZnNPs, GL-CuNPs, and GL-AgNPs toward 100 ppm of TMA are shown in Figure 8.

2.3. Gas-Sensing Mechanism. The sensing mechanism of the surface-modified cotton fabrics is based on the change in the chemi-resistance of the sensing element in the presence and absence of target vapors enabled by the electron-transfer dynamics during gas−solid adsorption/desorption processes. When the sensing element is exposed to ambient air atmosphere, oxygen molecules consume the electrons from the conduction band of the n-type semiconducting GL-AgNP sensing element. This adsorption reaction leads to the formation of O_2^- ions on the surface of the modified fabric, which in turn increases the surface resistance of the sensing element. The steady-state surface resistance was fixed as the baseline resistance (R_a). When the sensing element was exposed to the reducing type TMA, the interaction leads to desorption of oxygen ions from the sensing element enabled by the release of electrons from TMA. This process resulted in the increased charge carrier concentration, which in turn reduced the surface resistance. The steady-state surface resistance in the presence of target vapor was recorded as R_g. When the target vapor was released, the surface resistance again increased to the baseline value because of desorption of target vapor. The reaction mechanism is depicted in Figure 9. The response and recovery times of the GL-AgNP surface-modified cotton fabrics toward 100 ppm of TMA were found to be 114 and 66 s, respectively. The solid/vapor interaction scheme is given in eqs 2−4[48]

$$O_2(\text{atmosphere}) \leftrightharpoons O_2(\text{ads}) \quad (2)$$

$$O_2(\text{ads}) + e^-_{(\text{GL -AgNPs modified fabric})} \leftrightharpoons O_2^*(\text{ads})\ (\text{below } 100\ ^\circ\text{C}) \quad (3)$$

$$4(CH_3)_3N + 21O_{2(\text{ads})}^- \rightarrow 2N_2 \uparrow + 12CO_2 \uparrow + 18H_2O \uparrow + 21e^- \quad (4)$$

The transient response for 1−500 ppm of TMA of the GL-AgNPs surface-modified cotton fabric is shown in Figure 10a. The sensor response increased with the concentration of TMA and reached the maximum response of 2132 when the GL-AgNPs sensing element was exposed to 500 ppm. Figure 10b shows the response trend and linearity range of the GL-AgNPs surface-modified cotton fabric. Stability is one of the essential parameters for the gas sensor, and the response toward 100 ppm of TMA for 15 days is shown in Figure 11.

3. CONCLUSIONS

Biosphere faces serious threat with the emission of VOCs into the atmosphere from industries, solvent evaporation, petroleum products, and other human activities. Numerous health hazards occurring with the VOC emission have created the need for the VOC sensor development. In particular, TMA is

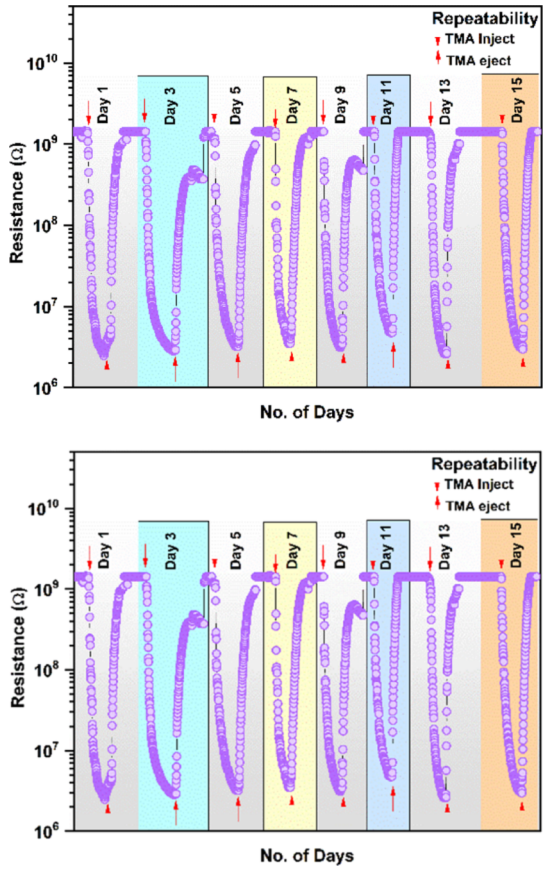

Figure 11. Repeatability trend of GL-AgNPs-modified fabric toward 100 ppm of TMA in different days.

https://dx.doi.org/10.1021/acsomega.9b02733
ACS Omega 2020, 5, 3839−3848

one of the VOCs that causes various health hazards including "trimethylaminuria" or "fish odor syndrome." Hence, there is a huge demand in the development of a new sensor material for TMA detection for use in food-processing industries, medical diagnosis, and environment. In this regard, for the first time, we have reported the formation of self-assembled silver-, copper-, and zinc-incorporated glycolipids, namely, GL-AgNPs, GL-CuNPs, and GL-ZnNPs by adding a solution of corresponding metal ions on to the gel formed by glycolipid **3** in 1,2-dichlorobenzene, which displays morphological transition from chiral helical tubules to fibrillar architecture without changing the phase. Morphological analysis of GL-NPs showed a 3D fibrous structure, which confirms the morphological transition in the gel induced by the interaction of metal ions with the coordination site of chiral helical tubules obtained from glycolipid **3**. The self-assembled silver-incorporated glycolipid further interacts with the cellulose of cotton fabric via H-bonding, resulting in the formation of hydrophobic fabric with a conducting property. The developed GL-AgNP-based fabric displayed a transient response for 1−500 ppm of TMA and a stable response toward 100 ppm of TMA for 15 days. The reported protocol based on the self-assembly process may open new avenues in sensor science. GL-AgNP-based flexible TMA sensor fabrics developed via the sequential self-assembly process hold great promise for various innovative applications in environmental science, healthcare, medicine, and biology. From the commercial point of view, GL-AgNP-based flexible fabrics shall be encapsulated in porous thermoplastic films such as Platilon U and Zitex G-104 without affecting the sensing performances such as selectivity, sensitivity, durability, and lifetime of the sensor.

4. EXPERIMENTAL SECTION

4.1. Materials and Methods. Reagents and solvents required for the synthesis of GL and GL-NPs were purchased from Alfa Aesar, Avra, Merck, SRL, TCI chemicals, and Sigma-Aldrich and used as such without any further purification. Compounds were purified using LR grade solvents, and distilled solvents were used when considered necessary. The progress of the reaction was monitored using thin-layer chromatography (TLC) on the 60G F_{254} precoated silica gel plates procured from Merck and visualized with the help of ultraviolet light or sulfuric acid spray or molecular iodine or *p*-anisaldehyde stain. ^{1}H- and ^{13}C-NMR spectra for the glycolipid were recorded on a Bruker AVANCE 300 MHz spectrometer at room temperature in dimethyl sulfoxide-d_6. Chemical shifts (δ) are reported with respect to the internal standard, tetramethylsilane, in parts per million (ppm), and coupling constants (J) are given in Hz. Proton multiplicity is assigned using the following abbreviations: singlet (s), doublet (d), triplet (t), quartet (q), and multiplet (m). Fourier transform infrared FTIR spectra of the cotton fabric, fabric coated with GL, and GL-NPs were recorded in the attenuated total reflectance mode using a PerkinElmer 100 FTIR spectrometer in the spectral range of 4000−500 cm^{-1}. Field emission scanning electron microscope integrated with an energy-dispersive X-ray system (JEOL, JSM-6701F, Japan) was used to observe the morphology of self-assembled GL, cotton fabric, and fabric coated with GL and GL-AgNPs. An X-ray photoelectron spectrometer (Thermo Fisher Scientific Inc., K-Alpha, USA) was used to record the XPS spectra of GL-AgNPs and were compared with those in our previously reported literature. XRD of GL-AgNPs, fabric, and fabric with GL-AgNPs was performed on a BRUKER-binary V3 diffractometer system, and the results were compared with native self-assembled GL.

4.2. Synthesis. *4.2.1. General Procedure for the Synthesis of Glycolipid GL 3.* Glycolipid GL **3** was synthesized from gluconolactone, hydrazine hydrate, and 2-hydroxy-4-pentadecylbenzaldehyde by following the procedure reported in the literature.[43] To a solution of gluconolactone (1.0 mmol) in ethanol, hydrazine hydrate (1.5 mmol) was added and refluxed for 30 min to form gluconolactone hydrazide. To the refluxed mixture, 2-hydroxy-4-pentadecylbenzaldehyde (1.0 mmol) was added and further refluxed for 90 min to produce glycolipid **3**. After completion of the reaction, as identified by TLC, the reaction mixture was cooled to room temperature. Upon cooling the reaction mixture, solid glycolipid **3** was precipitated, which was further filtered, washed well with cold ethanol, and air dried.

4.3. Preparation of Self-Assembled GL, GL-NPs, and GL-NP-Coated Cotton Fabric Material. A mixture of 1 mg of glycolipid, **GL 3**, and 1 mL of dichlorobenzene (1 mL) was taken in a glass vial and heated until the solid was completely dissolved. Upon cooling to room temperature, organogel formation was observed and confirmed by the "inversion of test tube" method. Further, self-assembled GL-AgNPs **4a**, GL-CuNPs **4b**, and GL-ZnNPs **4c**, generally referred as GL-NPs **4a−c**, were prepared by adding a solution of silver nitrate, copper acetate, and zinc acetate solution separately on to the gel. A slow percolation of these solutions in the gel matrix was observed by the change of color from transparent to black, green, and pale yellow, indicating the formation of self-assembled GL-NPs **4a−c**, respectively. Later, the left-over supernatant solution above the gel surface was decanted, and the sample was dried. The dried sample was thoroughly washed with aqueous EtOH (1:1 v/v), dried under vacuum, and stored in a desiccator for further studies. Self-assembled GL-NPs **4a−c** were coated on cotton by adopting the following procedure: Dried 10 mg of GL-NPs **4a−c** were completely dispersed in 25 mL of dichlorobenzene taken in a beaker by sonication for 10 min, followed by the immersion of a 5 × 5 cm cotton fabric with the help of a hanging clip, and left undisturbed for 24 h. After immersion, the fabric was removed and air dried for 48 h in a closed container for further studies. Our preliminary studies on the conductivity of self-assembled GL-AgNPs **4a**, GL-CuNPs **4b**, and GL-ZnNPs **4c** revealed that self-assembled GL-AgNPs **4a** are more promising and hence are further used for our investigation.

4.4. Rheological Analysis. The viscoelastic behavior, mechanical strength, thixotropic behavior, and processability of GL-AgNPs in gel form was investigated with a stress-controlled rheometer (Anton Paar 302 rheometer) equipped with steel-coated parallel-plate geometry (25 mm diameter). During the rheological analysis, the measurements were recorded by fixing a 1 mm gap between two parallel plates. Initially, linear viscoelastic range was obtained by performing the amplitude sweep measurement, which is directly proportional to the mechanical strength of the GL-AgNP gel sample. Then, frequency sweep was performed to examine the storage modulus G' and the loss modulus G'' as functions of frequency sweep from 0.1 to 300 rad s^{-1}.

4.5. Contact Angle Measurements. The hydrophobicity of fabric samples was investigated by contact angle measurements using a goniometer. The contact angle values reported

https://dx.doi.org/10.1021/acsomega.9b02733
ACS Omega 2020, 5, 3839−3848

are averages of three measurements made on different areas of the fabric surface.

4.6. Sensor Measurements. Sensing characteristics were investigated using a homemade chemical/gas testing chamber[44] integrated with a high-resistance electrometer (Keithley 6517 B, USA).

AUTHOR INFORMATION

Corresponding Authors

John Bosco Balaguru Rayappan − *Centre for Nano Technology & Advanced Biomaterials (CeNTAB) and School of Electrical & Electronics Engineering, SASTRA Deemed University, Thanjavur 613401, Tamil Nadu, India;* orcid.org/0000-0003-4641-9870; Email: rjbosco@ece.sastra.edu

Subbiah Nagarajan − *Department of Chemistry, School of Chemical and Biotechnology, SASTRA Deemed University, Thanjavur 613401, Tamil Nadu, India; Department of Chemistry, National Institute of Technology Warangal, Warangal 506004, Telangana, India;* orcid.org/0000-0003-2233-4872; Email: snagarajan@nitw.ac.in, snrajannpt@gmail.com

Authors

Ayyapillai Thamizhanban − *Department of Chemistry, School of Chemical and Biotechnology, SASTRA Deemed University, Thanjavur 613401, Tamil Nadu, India*

Guru Prasanth Sarvepalli − *Department of Chemistry, School of Chemical and Biotechnology and Centre for Nano Technology & Advanced Biomaterials (CeNTAB) and School of Electrical & Electronics Engineering, SASTRA Deemed University, Thanjavur 613401, Tamil Nadu, India*

Krishnamoorthy Lalitha − *Department of Chemistry, School of Chemical and Biotechnology, SASTRA Deemed University, Thanjavur 613401, Tamil Nadu, India;* orcid.org/0000-0002-5133-1614

Yadavali Siva Prasad − *Department of Chemistry, School of Chemical and Biotechnology, SASTRA Deemed University, Thanjavur 613401, Tamil Nadu, India*

Dinesh Kumar Subbiah − *Centre for Nano Technology & Advanced Biomaterials (CeNTAB) and School of Electrical & Electronics Engineering, SASTRA Deemed University, Thanjavur 613401, Tamil Nadu, India*

Apurba Das − *Department of Textile & Fibre Engineering, Indian Institute of Technology, New Delhi 110 016, India;* orcid.org/0000-0002-8141-6854

Complete contact information is available at: https://pubs.acs.org/10.1021/acsomega.9b02733

Author Contributions

The manuscript was written through contributions of all authors. All authors have given approval to the final version of the manuscript.

Notes

The authors declare no competing financial interest.

ACKNOWLEDGMENTS

Financial support from the Science and Engineering Research Board, Department of Science and Technology, India (sanction order no: CRG/2018/001386) and SPARC, Ministry of Human Resource Development, India (SPARC/2018−2019/P263/SL) is gratefully acknowledged. S.N. thanks the National Institute of Technology, Warangal for the infrastructure facilities. D.K.S. thanks the Council of Scientific & Industrial Research (CSIR), New Delhi for the Senior Research Fellowship (09/1095(0035)/18-EMR-1).

REFERENCES

(1) Makar, P. A.; Moran, M. D.; Scholtz, M. T.; Taylor, A. Speciation of Volatile Organic Compound Emissions for Regional Air Quality Modeling of Particulate Matter and Ozone. *J. Geophys. Res.* **2003**, *108*, 4041.

(2) Li, H.-Y.; Huang, L.; Wang, X.-X.; Lee, C.-S.; Yoon, J.-W.; Zhou, J.; Guo, X.; Lee, J.-H. Molybdenum Trioxide Nanopaper as a Dual Gas Sensor for Detecting Trimethylamine and Hydrogen Sulfide. *RSC Adv.* **2017**, *7*, 3680−3685.

(3) Ahn, J.-H.; Szulejko, J.; Kim, K.-H.; Kim, Y.-H.; Kim, B.-W. Odor and VOC Emissions from Pan Frying of Mackerel at Three Stages: Raw, Well-Done, and Charred. *Int. J. Environ. Res. Public Health* **2014**, *11*, 11753−11771.

(4) Szulczyński, B.; Gębicki, J. Currently Commercially Available Chemical Sensors Employed for Detection of Volatile Organic Compounds in Outdoor and Indoor Air. *Environments* **2017**, *4*, 21.

(5) Li, M.; Al-Sarraf, A.; Sinclair, G.; Frohlich, J. Fish Odour Syndrome. *Cmaj* **2011**, *183*, 929−931.

(6) Bain, M. A.; Faull, R.; Fornasini, G.; Milne, R. W.; Evans, A. M. Accumulation of Trimethylamine and Trimethylamine-N-Oxide in End-Stage Renal Disease Patients Undergoing Haemodialysis. *Nephrol., Dial., Transplant.* **2006**, *21*, 1300−1304.

(7) Sivalingam, D.; Gopalakrishnan, J. B.; Rayappan, J. B. B. Structural, Morphological, Electrical and Vapour Sensing Properties of Mn Doped Nanostructured ZnO Thin Films. *Sens. Actuators, B* **2012**, *166−167*, 624−631.

(8) Zhu, S.; Liu, X.; Chen, Z.; Liu, C.; Feng, C.; Gu, J.; Liu, Q.; Zhang, D. Synthesis of Cu-Doped WO_3 Materials with Photonic Structures for High Performance Sensors. *J. Mater. Chem.* **2010**, *20*, 9126−9132.

(9) Zamani, C.; Casals, O.; Andreu, T.; Morante, J. R.; Romano-Rodriguez, A. Detection of Amines with Chromium-Doped WO_3 Mesoporous Material. *Sens. Actuators, B* **2009**, *140*, 557−562.

(10) Ohashi, E.; Takao, Y.; fujita, T.; Shimizu, Y.; Egashira, M. Semiconductive Trimethylamine Gas Sensor for Detecting Fish Freshness. *J. Food Sci.* **1991**, *56*, 1275−1278.

(11) Bakır, M.; Karaaslan, M.; Dincer, F.; Delihacioglu, K.; Sabah, C. Tunable Perfect Metamaterial Absorber and Sensor Applications. *J. Mater. Sci.: Mater. Electron.* **2016**, *27*, 12091−12099.

(12) Perillo, P. M.; Rodríguez, D. F. Low Temperature Trimethylamine Flexible Gas Sensor Based on TiO2 Membrane Nanotubes. *J. Alloys Compd.* **2016**, *657*, 765−769.

(13) Heising, J. K.; van Boekel, M. A. J. S.; Dekker, M. Simulations on the Prediction of Cod (Gadus Morhua) Freshness from an Intelligent Packaging Sensor Concept. *Food Packag. Shelf Life* **2015**, *3*, 47−55.

(14) Takao, Y.; Fukuda, K.; Shimizu, Y.; Egashira, M. Trimethylamine-Sensing Mechanism of TiO2-Based Sensors 2. Effects of Catalytic Activity of TiO_2-Based Specimens on Their Trimethylamine-Sensing Properties. *Sens. Actuators, B* **1993**, *10*, 235−239.

(15) Takao, Y.; Iwanaga, Y.; Shimizu, Y.; Egashira, M. Trimethylamine-Sensing Mechanism of TiO2-Based Sensors 1. Effects of Metal Additives on Trimethylamine-Sensing Properties of TiO2 Sensors. *Sens. Actuators, B* **1993**, *10*, 229−234.

(16) Zou, B.; Wu, F.; Chen, C.; Ren, H.; Wang, Z.; Zou, L. Study on TMA-Sensing Properties of Nanocrystalline Titanium Dioxide Materials. *Sens. Actuators, B* **2006**, *119*, 370−373.

(17) Kwon, T. H.; Ryu, J. Y.; Choi, W. C.; Kim, S. W.; Park, S. H.; Choi, H. H.; Lee, M. K. Investigation on Sensing Properties of ZnO-Based Thin Film Sensors for Trimethylamine Gas. *Sens. Mater.* **1999**, *11*, 257−267.

(18) Nanto, H.; Tsubakino, S.; Kawai, T.; Ikeda, M.; Kitagawa, S.; Habara, M. Zinc Oxide Thin-Film Chemical Sensors in Conjunction

https://dx.doi.org/10.1021/acsomega.9b02733
ACS Omega 2020, 5, 3839−3848

with Neural Network Pattern Recognition for Trimethylamine and Dimethylamine Gases. *J. Mater. Sci.* **1994**, *29*, 6529−6532.
(19) Roy, S.; Basu, S. ZnO Thin Film Sensors for Detecting Dimethyl- and Trimethyl-Amine Vapors. *J. Mater. Sci.: Mater. Electron.* **2004**, *15*, 321−326.
(20) Pandeeswari, R.; Jeyaprakash, B. G. Nanostructured α-MoO_3 Thin Film as a Highly Selective TMA Sensor. *Biosens. Bioelectron.* **2014**, *53*, 182−186.
(21) Cho, Y. H.; Ko, Y. N.; Kang, Y. C.; Kim, I.-D.; Lee, J.-H. Ultraselective and Ultrasensitive Detection of Trimethylamine Using MoO_3 Nanoplates Prepared by Ultrasonic Spray Pyrolysis. *Sens. Actuators, B* **2014**, *195*, 189−196.
(22) Yang, S.; Liu, Y.; Chen, W.; Jin, W.; Zhou, J.; Zhang, H.; Zakharova, G. S. High Sensitivity and Good Selectivity of Ultralong MoO3 Nanobelts for Trimethylamine Gas. *Sens. Actuators, B* **2016**, *226*, 478−485.
(23) Deekshitha, M.; Nagarajan, V.; Chandiramouli, R. First-Principles Studies on Transport Property and Adsorption Characteristics of Trimethylamine on α-MoO_3 Molecular Device. *Chem. Phys. Lett.* **2015**, *641*, 129−135.
(24) Nishizaka, Y.; Yokoyama, C.; Inumaru, K.; Okuhara, T.; Misono, M. Effect of Additives and Particle Size on the Sensitivity of SnO_2-Based Sensors for Offensive-Odor Components. *Sens. Actuators, B* **1993**, *13*, 355−357.
(25) Wang, P.; Zheng, Z.; Cheng, X.; Sui, L.; Gao, S.; Zhang, X.; Xu, Y.; Zhao, H.; Huo, L. Ionic Liquid-Assisted Synthesis of α-Fe_2O_3 Mesoporous Nanorod Arrays and Their Excellent Trimethylamine Gas-Sensing Properties for Monitoring Fish Freshness. *J. Mater. Chem. A* **2017**, *5*, 19846−19856.
(26) Yang, T.; Wang, D.; Zhai, C.; Luo, Y.; Zhang, M. Ultrafast Response and Recovery of Single Crystalline α-Fe_2O_3 Nanorhombohedrons for Trimethylamine Sensing Applications. *Mater. Lett.* **2018**, *210*, 1−3.
(27) Park, S.-H.; Ryu, J.-Y.; Choi, H.-H.; Kwon, T.-H. Zinc Oxide Thin Film Doped with Al2O3, TiO2and V2O5as Sensitive Sensor for Trimethylamine Gas. *Sens. Actuators, B* **1998**, *46*, 75−79.
(28) Park, S.-H.; Ryu, J.-Y.; Choi, H.-H.; Kwon, T.-H. Zinc Oxide Thin Film Doped with Al2O3, TiO2 and V2O5 as Sensitive Sensor for Trimethylamine Gas. *Sens. Actuators, B* **1998**, *46*, 75−79.
(29) Park, S. H.; Choi, H. H.; Kwon, T. H. Semiconductor Sensors for Detecting TMA Gas. *Sens. Mater.* **1996**, *8*, 485−491.
(30) Zhang, W.-H.; Zhang, W.-D. Fabrication of SnO_2-ZnO Nanocomposite Sensor for Selective Sensing of Trimethylamine and the Freshness of Fishes. *Sens. Actuators, B* **2008**, *134*, 403−408.
(31) Woo, H.-S.; Na, C. W.; Kim, I.-D.; Lee, J.-H. Highly Sensitive and Selective Trimethylamine Sensor Using One-Dimensional ZnO-Cr_2O_3 Hetero-Nanostructures. *Nanotechnology* **2012**, *23*, 245501.
(32) Lee, C.-S.; Kim, I.-D.; Lee, J.-H. Selective and Sensitive Detection of Trimethylamine Using ZnO-In 2O3 Composite Nanofibers. *Sens. Actuators, B* **2013**, *181*, 463−470.
(33) Bien, C. E.; Chen, K. K.; Chien, S.-C.; Reiner, B. R.; Lin, L.-C.; Wade, C. R.; Ho, W. S. W. Bioinspired Metal-Organic Framework for Trace CO2 Capture. *J. Am. Chem. Soc.* **2018**, *140*, 12662−12666.
(34) Assfour, B.; Assaad, T.; Odeh, A. In Silico Screening of Metal Organic Framework for Iodine Capture and Storage. *Chem. Phys. Lett.* **2014**, *610*−*611*, 45−49.
(35) Tulchinsky, Y.; Hendon, C. H.; Lomachenko, K. A.; Borfecchia, E.; Melot, B. C.; Hudson, M. R.; Tarver, J. D.; Korzyński, M. D.; Stubbs, A. W.; Kagan, J. J.; et al. Reversible Capture and Release of Cl2 and Br2 with a Redox-Active Metal-Organic Framework. *J. Am. Chem. Soc.* **2017**, *139*, 5992−5997.
(36) Martín-Calvo, A.; Lahoz-Martín, F. D.; Calero, S. Understanding Carbon Monoxide Capture Using Metal-Organic Frameworks. *J. Phys. Chem. C* **2012**, *116*, 6655−6663.
(37) Liang, L.; Liu, C.; Jiang, F.; Chen, Q.; Zhang, L.; Xue, H.; Jiang, H. L.; Qian, J.; Yuan, D.; Hong, M. Carbon Dioxide Capture and Conversion by an Acid-Base Resistant Metal-Organic Framework. *Nat. Commun.* **2017**, *8*, 1233.
(38) Duan, J.; Pan, Y.; Liu, G.; Jin, W. Metal-Organic Framework Adsorbents and Membranes for Separation Applications. *Curr. Opin. Chem. Eng.* **2018**, *20*, 122−131.
(39) Hromadka, J.; Tokay, B.; Correia, R.; Morgan, S. P.; Korposh, S. Highly Sensitive Volatile Organic Compounds Vapour Measurements Using a Long Period Grating Optical Fibre Sensor Coated with Metal Organic Framework ZIF-8. *Sens. Actuators, B* **2018**, *260*, 685−692.
(40) Sharma, N.; Sharma, N.; Srinivasan, P.; Kumar, S.; Balaguru Rayappan, J. B.; Kailasam, K. Heptazine Based Organic Framework as a Chemiresistive Sensor for Ammonia Detection at Room Temperature. *J. Mater. Chem. A* **2018**, *6*, 18389−18395.
(41) Yamagiwa, H.; Sato, S.; Fukawa, T.; Ikehara, T.; Maeda, R.; Mihara, T.; Kimura, M. Detection of Volatile Organic Compounds by Weight-Detectable Sensors Coated with Metal-Organic Frameworks. *Sci. Rep.* **2015**, *4*, 6247.
(42) Chidambaram, A.; Stylianou, K. C. Electronic Metal-Organic Framework Sensors. *Inorg. Chem. Front.* **2018**, *5*, 979−998.
(43) Lalitha, K.; Sridharan, V.; Maheswari, C. U.; Vemula, P. K.; Nagarajan, S. Morphology transition in helical tubules of a supramolecular gel driven by metal ions. *Comm* **2017**, *53*, 1538−1541.
(44) Shankar, P.; Rayappan, J. B. B. Racetrack Effect on the Dissimilar Sensing Response of ZnO Thin Film-An Anisotropy of Isotropy. *ACS Appl. Mater. Interfaces* **2016**, *8*, 24924−24932.
(45) Cook, T. R.; Zheng, Y.-R.; Stang, P. J. Metal-Organic Frameworks and Self-Assembled Supramolecular Coordination Complexes: Comparing and Contrasting the Design, Synthesis, and Functionality of Metal-Organic Materials. *Chem. Rev.* **2013**, *113*, 734−777.
(46) Xu, Q.; Xie, L.; Diao, H.; Li, F.; Zhang, Y.; Fu, F.; Liu, X. Antibacterial Cotton Fabric with Enhanced Durability Prepared Using Silver Nanoparticles and Carboxymethyl Chitosan. *Carbohydr. Polym.* **2017**, *177*, 187−193.
(47) Babu, K. F.; Dhandapani, P.; Maruthamuthu, S.; Kulandainathan, M. A. One Pot Synthesis of Polypyrrole Silver Nanocomposite on Cotton Fabrics for Multifunctional Property. *Carbohydr. Polym.* **2012**, *90*, 1557−1563.
(48) Subbiah, D. K.; Babu, K. J.; Das, A.; Rayappan, J. B. B. NiOx Nanoflower Modified Cotton Fabric for UV Filter and Gas Sensing Applications. *ACS Appl. Mater. Interfaces* **2019**, *11*, 20045−20055.
(49) Rajasekharan, T.; Seshubai, V. On the electrical conductivity of transition metals. *Cond-Mat.Mtrl-Sci.* **2011**, arXiv:1102.5654v1.

https://dx.doi.org/10.1021/acsomega.9b02733
ACS Omega 2020, 5, 3839−3848